

International Journal of  
**Applied  
Ceramic  
TECHNOLOGY**

Ceramic Product Development and Commercialization

## **Integrally Cored Ceramic Mold Fabricated by Ceramic Stereolithography**

**Chang-Jun Bae and John W. Halloran\***

*Department of Materials Science and Engineering, University of Michigan, Ann Arbor,  
Michigan 48109-2136*

Ceramic stereolithography (SLA) was used to fabricate a ceramic investment casting mold with the integral core within a ceramic mold shell, produced in a single patternless construction from refractory-grade fused silica. The SLA build material was a photopolymerizable suspension of 60 vol% fused silica dispersed in a monomer solution based on 1,6-hexanediol diacrylate. The mold had 1047 layers, each 100  $\mu\text{m}$  thick. Green body dimensions before sintering were approximately 0.7% smaller than the design within the plane of the layers, and approximately 0.3% larger than the design perpendicular to the layers. The sintering shrinkage was  $10.7 \pm 0.2\%$  in both directions.

### **Introduction**

The superalloy airfoils in gas turbine engines have hollow structures with complex interior cooling passages.<sup>1</sup> These complex hollow airfoils are produced using investment casting<sup>2</sup> which involves multiple steps to separately prepare the ceramic core, which is then inserted into the mold for the exterior shell. For example, one set of injection molding tooling is required to fabricate the com-

plex ceramic cores, and a separate set injection molding tooling is needed to mold the wax pattern around the ceramic core. To make the ceramic shell mold, the wax pattern containing a ceramic core is repeatedly dipped in ceramic slurry, coated with coarse refractory stucco, and dried before the next layer is applied.<sup>3</sup> These steps can be eliminated if a single process is capable of directly producing a mold that has the casting cavity integrated with the ceramic core, or an integrally cored ceramic mold (ICCM).<sup>4</sup> In this work, we demonstrate an ICCM that combines the ceramic core with a ceramic shell mold in a single patternless construction, as shown in Fig. 1.

Such a complex design can be built from many layers using a solid freeform fabrication technique<sup>5</sup> in which sophisticated three-dimensional (3D) objects are

This work was supported by the Office of Naval Research under Grant N00421-06-1-0002, and conducted as part of a collaboration with Mr. Wil Baker of Honeywell and PCC Airfoils, PLC.

\*peterjon@umich.edu

© 2010 The American Ceramic Society

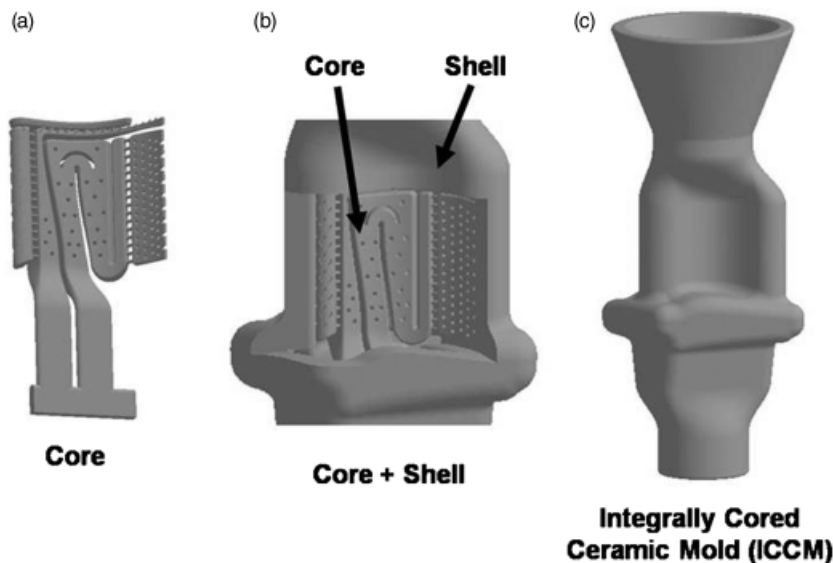


Fig. 1. The designs of ceramic mold for superalloy airfoil: (a) Ceramic core for the complex internal cooling passages, (b) the cross-section of the pattern section, and (c) the design of integrally cored ceramic mold.

produced directly from a layer-by-layer process based on computer-aided design (CAD) files. Stereolithography (SLA) is the most commercialized technique among the solid freeform fabrication processes because it can produce 3D objects with close dimensional tolerances and good surface finish.<sup>6</sup> Conventional SLA builds polymeric parts, but the technique has been extended to ceramic stereolithography (CerSLA), which is able to produce 3D ceramic objects.<sup>7–9</sup> CerSLA is a repeated layered manufacturing process where thin liquid layers of ceramic-monomer suspension are solidified by photopolymerization with a UV laser, thereby “writing” the design for each slice. This process can be conducted with a variety of powders and photopolymerizable media.<sup>10,11</sup> Metal casting molds have been built by SLA from silica,<sup>12</sup> including complex molds with integral cores.<sup>13</sup> In this paper, we report the fabrication of a silica refractory ICCM by CerSLA, and describe the processing technique with emphasis on the accuracy of the fabrication.

## Experimental Procedure

### Suspension Preparation

The photopolymerizable suspension was prepared by dispersing ceramic powders in a solution of acrylate

monomers. The monomer mixture was a blend of 87.5 weight percent of a difunctional monomer 1,6-hexanediol diacrylate (HDDA, SR238) and 12.5 weight percent of a tetrafunctional monomer ethoxylated pentaerythritol tetraacrylate (EPTA, SR494), both used as received from Sartomer company (Exton, PA). A photoinitiator, 1-hydroxy cyclohexyl phenyl ketone (Irgacure 184, Ciba Specialty Chemicals, Tarrytown, NY) was used to initiate the polymerization reaction of monomer mixtures. The design principles for photopolymerizable ceramic suspensions are presented elsewhere.<sup>14</sup> The ceramic powder was a refractory silica ( $\text{SiO}_2$ , PCC airfoils, Sanford, NC), consisting of irregular glassy milled fused silica (density of  $2.2 \text{ gm/cm}^3$ ), with an average size range of  $3 \mu\text{m } d_{10}$ ,  $12 \mu\text{m } d_{50}$ , and  $66 \mu\text{m } d_{90}$ . To prepare a colloiddally stable dispersion of the silica in the acrylates, a quaternary amine dispersant (Variquat CC-59, Goldschmidt, Hopewell, VA) was added in an amount equal to 3% of the weight of the  $\text{SiO}_2$  powder. In order to prepare the ceramic suspension,  $\text{SiO}_2$  powder and dispersant were gradually mixed into the monomer mixtures without a photoinitiator. Up to a solid loading of 50 vol%, the suspension was mixed and homogenized in a high-speed shear mixer for 5 min. At a solid loading of 60 vol%, more time was required for the dispersants to adsorb and colloiddally

stabilize the suspension so that the mixtures were ball milled for 24 h. The photoinitiator, at a concentration of 2 wt% with respect to the monomer, was added to a 60 vol% suspension and the final mixture was ball milled again for 2 h. Bubbles were removed from the completed suspension by vacuum deairing. The suspension was slightly shear thinning, with an apparent viscosity of 0.58 Pa s at a shear rate of  $10 \text{ s}^{-1}$ . Further characteristics are reported elsewhere.<sup>4</sup>

### Fabrication of ICCM using CerSLA

A 3D green mold was fabricated using a commercial SLA apparatus (SLA-250, 3D Systems Inc. Valencia CA) with a UV laser. The laser was a diode pumped solid-state laser (Xcyte CY-SM60, JDS Uniphase, Milpitas, CA), which had a quasicontinuous wave emitting at 355 nm. The output power was 40 mW with a beam diameter of 125  $\mu\text{m}$ . CAD files (in STL format) were prepared for SLA using the software 3D Lightyear 1.5.2 (3D Systems Inc.). This program assigns build parameters to the part and then slices the file into horizontal layers for building. The SLA 250 builds the mold by first applying a 100- $\mu\text{m}$ -thick layer of liquid photopolymerizable suspension, next the laser scans the surface of the liquid monomer in the specified pattern for that layer, thus solidifying the surface of the suspension in predefined areas. The regions exposed to the laser are now small sections of green ceramic, consisting of the silica powder in a polyacrylate binder. When the layer is finished, after about 1 s, the support platform and first layer move downward into the vat of liquid monomer resin. The liquid monomer flows across the first polymerized layer, and then takes 40 s of stabilizing time to make a flat surface of suspension. The laser scans this new surface, polymerizing the second layer. This process is repeated for subsequent layers, up to the 1047 layers required for this ICCM. When part building is carried out, the part is a green body of silica in polyacrylate binder. After SLA fabrication, the cured part is removed from the rest of the uncured suspension and rinsed in isopropyl alcohol for 20 min. The polymer in the green body is removed in a binder burnout process consisting of several controlled heating steps up to 600°C. This temperature is maintained for 2 h, and then the burned part is sintered at 1300°C for 30 min in air. Details of the binder burnout and sintering procedure are reported elsewhere.<sup>4</sup>

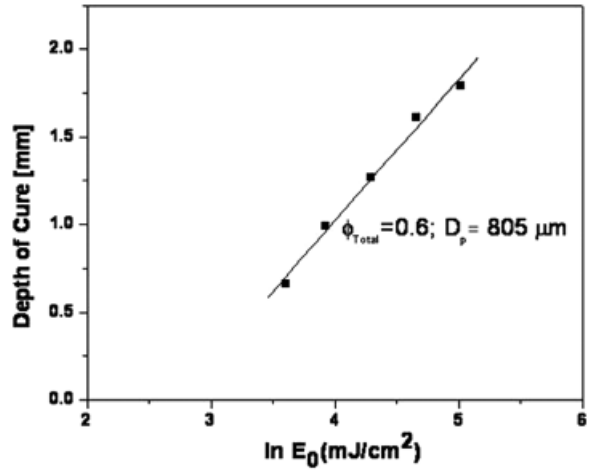


Fig. 2. Depth of cure as a function of energy dose measured using WINDOWPANE technique on the suspension including 60 vol% of fused silica. The resin sensitivity ( $D_p$ ) and critical energy dose ( $E_c$ ) calculated using Eq. 1 are  $805 \pm 48 \text{ mm}$  and  $15.33 \pm 1.29 \text{ mJ/cm}^2$ , respectively.

### Photopolymerization Parameters

For photopolymerization, the suspension is illuminated by the specific energy dose  $E$  ( $\text{mJ/cm}^2$ ), which is designed to cure the suspension to the desired cure depth  $C_d$ . Dose and cure depth are related through two properties of the photopolymerizable suspension: critical energy dose ( $E_c$ ) and sensitivity ( $D_p$ ) by<sup>6,14</sup>:

$$C_d = D_p \ln \left( \frac{E}{E_c} \right) \quad (1)$$

where  $E$  is the exposure energy dose delivered to the surface and  $C_d$  is the thickness of a cured layer at energy  $E$ . The critical energy dose ( $E_c$ ) and sensitivity ( $D_p$ ) were determined by measuring the cure depth  $C_d$  of small coupons at five different energy doses ( $E$ ). Figure 3 shows a cure depth versus the logarithm of energy dose. The resin sensitivity  $D_p$  (the distance at which the laser intensity is reduced by  $1/e$ ) is obtained from the slope in Fig. 2 and the critical energy dose  $E_c$  is obtained from the intercept. To build 100-mm-thick layers, the processing parameters were  $D_p$  of 805  $\mu\text{m}$  and  $E_c$  of  $15 \pm 1.29 \text{ mJ/cm}^2$ . To insure joining between the layers, the overcure was 25%, and hence the cure depth was 125  $\mu\text{m}$ .

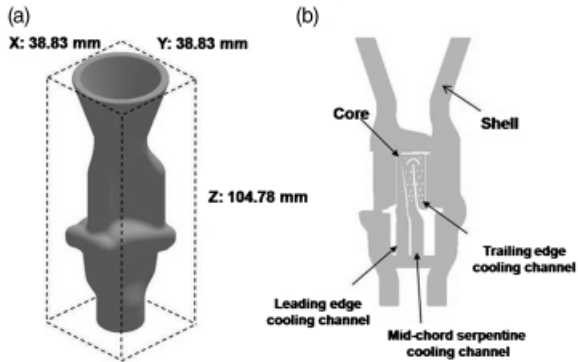


Fig. 3. Overall dimensions of integrally cored ceramic mold (ICCM) fabricated by ceramic stereolithography; (a) the size of ICCM and (b) the cross-section of ICCM showing core, shell parts, and three cooling channels; leading edge cooling channel, midchord serpentine cooling channel, and trailing edge cooling channel.

## Results and Discussion

### ICCM for Turbine Airfoil Design and Fabrication

The ICCM is composed of core, casting cavity, and shell parts, where the core generates internal cooling passages of a turbine airfoil. Figure 3a shows the exterior of the ICCM design with overall dimensions of  $38.83 \text{ mm} \times 38.83 \text{ mm} \times 104.78 \text{ mm}$  ( $X \times Y \times Z$ ) for fabricating a turbine airfoil. Figure 3b is a cross-section showing the shell section (defining the outside metal surface) and the core section (defining the interior cooling passage). The internal features in the ICCM contain three intricate cooling channels that form a cooling system. The channels are a leading edge cooling channel, a midchord serpentine cooling channel, and a trailing edge cooling channel. To allow the core to be visualized, a “window” was built on the concave side of the mold to reveal the core inside. Metal gap thickness is as small as 0.5 mm on suction and pressure side. The core serpentine and flag has 0.56 mm holes, with 0.56 mm flag connector posts.

In order to generate each layer of the ICCM, the CAD file is sliced into horizontal layers. The ICCM was sliced with a layer thickness of  $100 \mu\text{m}$  so that 1047 layers were generated based on the Z height of 104.7 mm. Figure 4b shows five of these layers, where the initial root of the core is created in layer 400, and several passageways between the core and shell mold developed between layers 400 and 800. Although it only takes about 5 s to write a single layer, it requires about

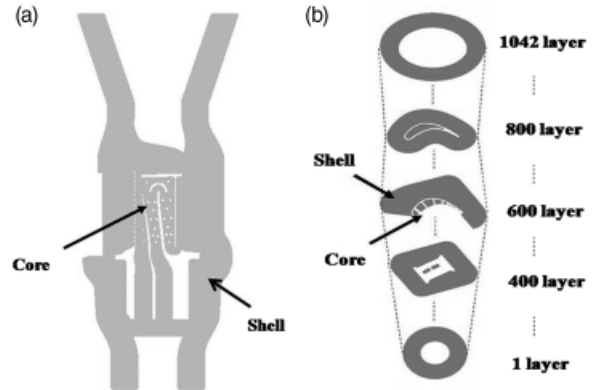


Fig. 4. Integrally cored ceramic mold (ICCM); (a) the vertical cross-section of ICCM showing core and shell parts and (b) the five horizontal cross-sections among 1047 layers of ICCM, which was sliced with a layer thickness of  $100 \mu\text{m}$ .

5.5 h to build the green body of ICCM up to 400 layers, with most time spent in the recoating step.

Given the sliced layers in Fig. 4b, the cross-section of STL file and a green body of ICCM are shown in Fig. 6. The positions of layers 400 and 630 are indicated by the dashed lines on the vertical cross-section shown in Fig. 5. Figure 5a shows the cross-section of the 630th layer, including three different core parts in the green body. They will turn into three cooling channels: leading edge, midchord serpentine, and trailing edge cooling channels. Symbols A–A' to D–D' are used to compare the dimensional accuracy between STL file and green body on the X–Y plane. At the 400th layer shown in Fig. 5b, two separated parts are growing in the core region.

A gap is left between the core and shell, which is filled with metal during casting, as shown in Fig. 6a. The gap is designed to be 0.5 mm. When an ICCM is produced via exposure to ultraviolet radiation on the suspension, the optimized photopolymerization processing parameters,  $D_p$  805  $\mu\text{m}$  and  $E_c$  15  $\text{mJ}/\text{cm}^2$ , were used to produce the gap. As shown in Fig. 6b, the green body with the resolved gap was successfully fabricated between core and shell. At the positions of cross-section, the gap sizes of the green body are fairly controlled under  $\pm 30 \mu\text{m}$ .

### Microstructure of Sintered Silica Molds

As this is a layered manufacturing process, the integrity of the interfaces between the layers is critical. Inappropriate choice of building parameters can lead to

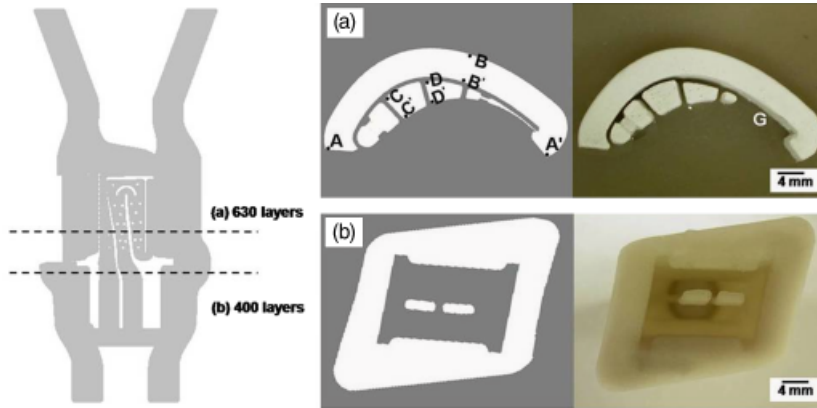


Fig. 5. Accuracy of the integrally cored ceramic mold (ICCM) built by ceramic stereolithography. (a) STL file and green body of ICCM with core and shell mold at the layer number 630th (A–A' to D–D', measured length; G, missing part) and (b) STL file and green body of ICCM with core and shell mold at the layer number 400th.

cracking and delamination after sintering.<sup>15</sup> For this porous refractory silica, the mechanical integrity depends upon avoiding cracks. The flexural strength depends on the sintering temperature and amount of devitrification of the fused silica to form cristobalite. The materials presented here were sintered at 1300°C

and had about 25 vol% cristobalite, and hence had a flexural strength on the order of 12 MPa (C-J Bae and J. W. Halloran, unpublished data).

Figure 7 shows a typical microstructure of the as-fired surface and a fracture surface of the ICCM. Figure 7a shows the exterior as-fired surface, with the layering

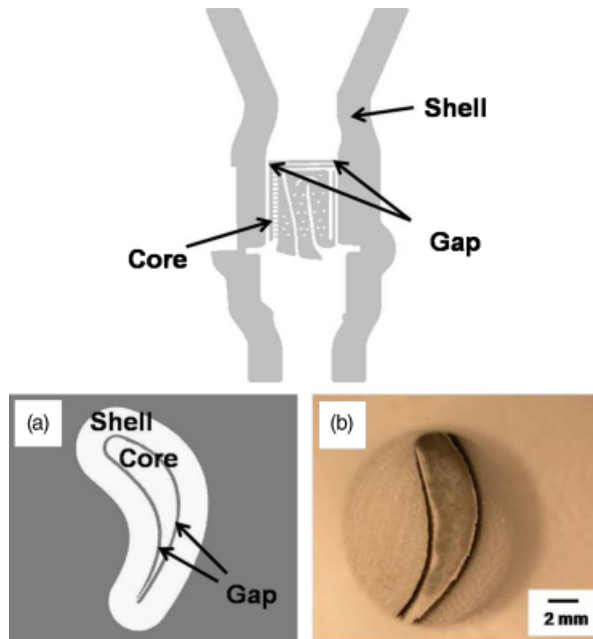


Fig. 6. Gap between core and shell for the cast metal; (a) the design of gap and (b) gap resolved in the green body of integrally cored ceramic mold.

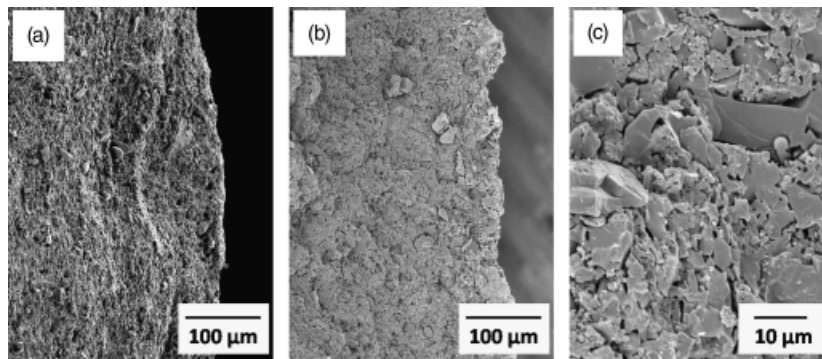


Fig. 7. SEM images of microstructure of the sintered silica mold, layering direction is horizontal; (a) as-fired surface, (b) low-magnification image of fracture surface, with field of view including four layers, and (c) high-magnification image of fracture surface of integrally cored ceramic mold.

direction horizontal and the build direction vertical. The field of view includes at least four of the 100  $\mu\text{m}$  layers, but these layers are not obvious on the surface of the build. The roughness of the surface is controlled by a few large particles of  $\sim 60 \mu\text{m}$ . The powder consisted of irregular glassy milled fused silica having a  $d_{90}$  of 66  $\mu\text{m}$ . The fracture surface appears in Fig. 7b, with a field of view including at least four layers. There is no clear evidence of the layering, and no evidence of delamination or cracks. Figure 7c illustrates the microstructure on a finer scale, showing that the larger fused silica particles are bonded by a matrix of finer silica.

### Resolution and Accuracy Issues in CerSLA

Consistency and accuracy are important factors that should be considered when integrally cored ceramic molds (ICCM) are fabricated using CerSLA. For example, ceramic shell molds are required to have a constant thickness for strength and predictable thermal behaviour to avoid mold failure during metal casting.<sup>4</sup> In addition, for consistent and accurate cast metal, the consistency and accuracy of green bodies affect those of sintered bodies. If the ICCM green bodies are produced within dimensional tolerances, the CerSLA process will be able to replace the conventional investment casting process. Linear dimensional tolerances of about  $\pm 0.15$ – $0.25 \text{ mm}/25 \text{ mm}$  (6–10 mil/in.) are typical for conventional investment casting.<sup>3</sup>

In order to evaluate how accurately CerSLA can build an ICCM, the sizes of specific features were measured and compared between the CAD design, green body, and sintered ceramic body. These measurements

were performed on four samples, which were only built to layer 630. Figure 5a shows an STL file including core and shell parts, representing a cross-section of the layer in a targeted ICCM and the cross-section of a green body composed of polymer and ceramic material fabricated by CerSLA, respectively. Symbols A–A' to D–D' in Fig. 5a and E–E' to F–F' in Fig. 8a indicate positions in X–Z measured in each sample to evaluate the accuracy of CerSLA, respectively. Given the STL file of the layer, the size difference of green and sintered body (not shown) and shrinkage factor is compared and calculated. Table I displays the size difference resulting from the comparison between a green and a sintered body with the STL file, for both core and shell parts of the cross-section of layer 630. The green body features, which could be more accurately measured, were about  $0.7 \pm 0.3\%$  smaller than the STL dimensions of the design within the X–Y plane, and in the Z-direction were 0.15–0.4% larger in the green body than in the STL design. The sintering shrinkage in the X–Y plane was  $10.8 \pm 0.1\%$  and  $10.65 \pm 0.05\%$  in the Z-direction, which are similar.

Figure 8 demonstrates images showing a full-size integrally cored ceramic mold: STL file (Fig. 8a), the green mold (Fig. 8b), and the sintered mold (Fig. 8c). After removing the polyacrylate binder, and sintering at  $1300^\circ\text{C}$  for 30 min, the sintered mold can be produced without any cracks in the shell or core. However, the finest features of the design are missing in the green and sintered part. Position G shown in Figs 5a and 8b, c represents the trailing edge cooling channel parts. These are connected to the larger features by a series of 0.56 mm posts and thin down to 0.38 mm at the tip.

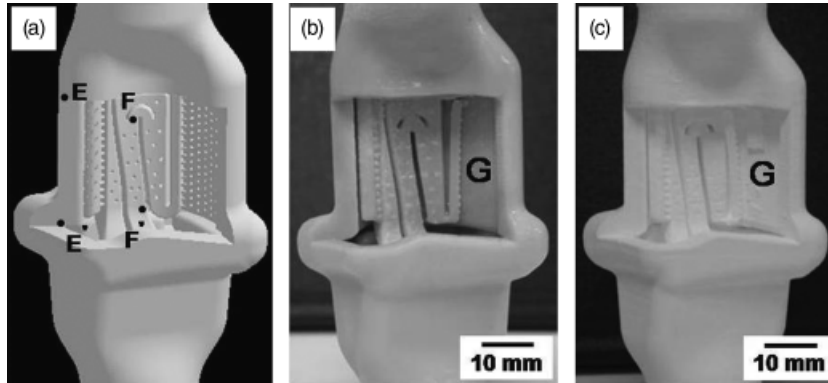


Fig. 8. Integrally cored ceramic mold for turbine airfoil with a complex internal hollow structure fabricated using ceramic stereolithography: (a) STL file, (b) green body, and (c) sintered body without any cracks at core and shell parts (E–E' and F–F': measured).

Table I. Evaluation on Accuracy of CerSLA from the Comparison between STL File and Green Body of ICCM

Axis	Part	As-built before sintering (mm)		After sintering (mm)	
		STL file	Green body	Sintering shrinkage (%)	Sintered body
X–Y	A–A'	33.6	33.37 ± 0.11	10.8	29.72 ± 0.07
	B–B'	4.66	4.42 ± 0.11	10.9	3.93 ± 0.07
	C–C'	4.72	4.60 ± 0.1	10.7	4.11 ± 0.08
	D–D'	3.89	3.87 ± 0.09	10.9	3.45 ± 0.04
Z	E–E'	26.67	26.71 ± 0.17	10.6	23.91 ± 0.05
	F–F'	22.72	22.81 ± 0.07	10.7	20.36 ± 0.04

CerSLA, ceramic stereolithography; ICCM, integrally cored ceramic mold.

We suspect that these fine features were not fully resolved during building with the laser beam, which had a 0.125 mm focal point. These features may have broken away after building, when the uncured suspension is drained and the mold interior was rinsed with isopropanol.

## Conclusion

CerSLA was used to fabricate a 104-mm-tall ceramic investment casting mold with the integral ceramic core within a ceramic mold shell, produced in a single patternless construction from refractory-grade fused silica. The SLA build material was a photopolymerizable suspension of 60 vol% fused silica dispersed in a monomer solution based on 1,6-hexanediol diacrylate. The mold had 1047 layers, each 100 μm thick. Fine features of the internal airfoil core were re-

solved, although the finest trailing edge features were not resolved. For the green body before sintering, the dimension in the X–Y plane was approximately 0.7% smaller than the design, while dimensions in the Z-direction were approximately 0.3% larger than the design. The sintering shrinkage was 10.7 ± 0.2% in both directions.

## References

1. C. F. Caccavale and W. E. Sikkenga, "Investment Casting Using Core with Integral Wall Thickness Control Means," U.S. Patent 5296308, 1994.
2. C. M. Cheah, C. K. Chua, C. W. Lee, C. Feng, and K. Totong, "Rapid Prototyping and Tooling Techniques: A Review of Applications for Rapid Investment Casting," *Int. J. Adv. Manuf. Technol.*, 25 [3–4] 308–320 (2005).
3. P. R. Beeley and R. F. Smart, *Investment Casting*, 65–78. Cambridge University Press, Cambridge, U.K., 1995.
4. C.-J. Bae, "Integrally Cored Ceramic Investment Casting Mold Fabricated by Ceramic Stereolithography," Ph.D. Thesis, University of Michigan, Ann Arbor, 2008.
5. J. W. Halloran, C.-J. Bae, C. Torres-Garibay, V. Tomeckova, S. Das, and W. Baker, "Manufacture of Complex Ceramics by Photopolymerization," *Global Roadmap for Ceramics—ICC2, Proceedings, the Proceedings of the 2nd*

- International Congress on Ceramics, ISBN 978-88-8080-084-2*, Verona, Italy, June 29–July 4, 2008, eds., Alida Bellosi, and G. Nicola Babini. Agenzia Polo Ceramico S.C. A.r.l., Faenza, Italy, 369–378, 2008.
6. P. F. Jacobs, *Rapid Prototyping & Manufacturing—Fundamentals of Stereolithography*, 397–450. SME, La Crescenta, CA, 1992.
  7. F. Doreau, C. Chaput, and T. Chartier, “Stereolithography for Manufacturing Ceramic Parts,” *Advanced Engineering Materials*, 2 [8] 493–494 (2000).
  8. T. Chartier, C. Chaput, F. Doreau, and M. Loiseu, “Stereolithography of Structural Complex Ceramic Parts,” *J. Mater. Sci.*, 37 3141–3147 (2002).
  9. M. L. Griffith and J. W. Halloran, “Freeform Fabrication of Ceramics Via Stereolithography,” *J. Am. Ceram. Soc.*, 79 [10] 2601–2608 (1996).
  10. Y. De Hazan, J. Heinecke, A. Weber, and T. Graule, “High Solids Loading Ceramic Colloidal Dispersions in UV curable media with via Comb-Polyelectrolyte Dispersants,” *J. Colloid Interface Sci.*, 337 [1] 66–74 (2009).
  11. W. Zhou, D. Li, and H. Wang, “A Novel Aqueous Suspension for Ceramic Stereolithography,” *Rapid Prototyping J.*, 16 [1] 29–35 (2010).
  12. C. Esposito Corcione, A. Greco, F. Mongagna, A. Licciulli, and A. Maffezzoli, “Silica Moulds Built by Stereolithography,” *J. Mater. Sci.*, 40 4899–4904 (2005).
  13. D. J. Frasier, M. Kush, M. E. Schlienger, and M. Baldwin, “Method and Apparatus for Production of a Cast Component,” U.S. Patent 6932145, 2005.
  14. V. Tomeckova and J. W. Halloran, “Predictive Models for the Photopolymerization of Ceramic Suspensions, JECS 7799,” *J. Eur. Ceram. Soc.*, 30 2833–2840 (2010).
  15. C.-J. Bae and J. W. Halloran, “Influence of Residual Monomer on Cracking in Ceramics Fabricated by Ceramic Stereolithography,” *International Journal of Applied Ceramic Technology*, (2010), in press.